THE JOURNAL OF PHYSICAL CHEMISTRY Letters

Letter

pubs.acs.org/JPCL

Luminescence Properties of Compressed Tetraphenylethene: The Role of Intermolecular Interactions

Hongsheng Yuan,[†] Kai Wang,[†] Ke Yang,[‡] Bingbing Liu,[†] and Bo Zou*[,†]

[†]State Key Laboratory of Superhard Materials, Jilin University, Qianjin Street 2699, Changchun 130012, China

[‡]Shanghai Institute of Applied Physics, Chinese Academy of Sciences, 239 Zhang Heng Road, Shanghai 201203, China

Supporting Information

ABSTRACT: Mechanochromic materials with aggregation-induced enhanced emission (AIEE) characteristic have been intensively expanded in the past few years. In general, intermolecular interactions invariably alter photophysical processes, while their role in the luminescence properties of these AIEE-active molecules is difficult to fully recognize because the pressurized samples possess amorphous nature in many cases. We now report the high-pressure studies on a prototype AIEE-active molecule, tetraphenylethene, using diamond anvil cell technique with associated spectroscopic measurements. An unusual pressure-dependent color, intensity, and lifetime change in tetraphenylethene has been detected by steady-state photoluminescence and time-resolved emission decay measurements. The flexible role of the aromatic C−H···π and C−H···C contacts in structural recovery, conformational modification, and emission efficiency modulation upon compression is demonstrated through structure and infrared analysis.

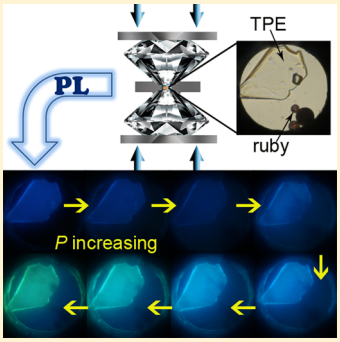

SECTION: Spectroscopy, Photochemistry, and Excited States

The development of luminescent materials sensitive to mechanical stimuli has gained wide attention due to their promising applications in fluorescent switches and optical devices.[1−5] However, most luminogens suffer from the notorious aggregation-caused quenching effect in the condensed phase, which hampers their real-world applications in an engineering robust form. Instead of preventing the natural process of chromophore aggregation, Park and Tang observed an unusual phenomenon of aggregation-induced enhanced emission (AIEE): cyano stilbene derivatives and propeller-shaped luminogens such as silole and tetraphenylethene (TPE) are induced to emit intensely by aggregate formation.[6−9] (Note that the term "aggregation-induced emission (AIE)" is adopted for the molecules including silole and TPE that are non-luminescent in the solution state but emissive in the aggregate state.[8,9] In our opinions, the term "AIE" can be covered by the term "AIEE" in a board sense. For simplicity, we only use the term "AIEE" hereafter.) Importantly, many ground AIEE-active luminogens with amorphous nature are reported to emit redder lights than their crystalline counterparts, thus making these luminogens with mechanochromic property.[1,2,10,11] Recently, Zhang and Tang et al. fabricated a series of mechanochromic AIEE-active luminogens with high contrast and high efficiency by virtue of effective intermolecular interactions, such as C−H···π, C−H···O, and C−H···N contacts.[12,13] In view of this, an in-depth understanding of the relationship between the photophysical properties and the packing styles involving intermolecular interactions is urgently desirable and of great importance in the era.

Numerous studies showed that applying external stress by diamond anvil cell (DAC) technique in conjunction with spectroscopic measurements is a powerful method to offer an in situ investigation on structural modifications.[14−19] In particular, hydrogen-bonding evolution under pressure has drawn considerable interest in the soft functional materials recently.[20−23] TPE is a prototype AIEE-active chromophore with highly twisted conformations, which is locked by multiple aromatic C−H···π and C−H···C contacts.[24,25] These weak contacts are thus expected to be modulated by extreme compression with associated changes in the spectroscopic properties, especially photoluminescence (PL). We now report the high-pressure response of TPE up to 10 GPa using DAC technique. The results demonstrate the important role of intermolecular interactions in modulating the PL properties in the AIEE-active luminogens.

Under ambient conditions, solid-state TPE exhibited a deep-blue emission with the maximum wavelength (λ_{em}) of 448 nm. The excitation spectrum revealed the good excitation wavelength λ_{ex} ranging from 370 to 405 nm (Figure S7, Supporting Information). During the compression process, the PL maximum gradually red-shifted to 467 nm (sky blue) at 5.3 GPa and eventually to 488 nm (spring green) at 10 GPa (Figure 1 and Figure S3, Supporting Information). In general, the pressure-induced conformational planarization is responsible for the red shift in PL spectra of luminogens. It is intriguing to note that there is a larger red shift of TPE crystals in PL spectra when the pressure is over ∼4 GPa (Figure 1a), indicating that the conformational planarization is augmented.

Received: July 2, 2014
Accepted: August 18, 2014
Published: August 18, 2014

   dx.doi.org/10.1021/jz501371k | J. Phys. Chem. Lett. 2014, 5, 2968−2973

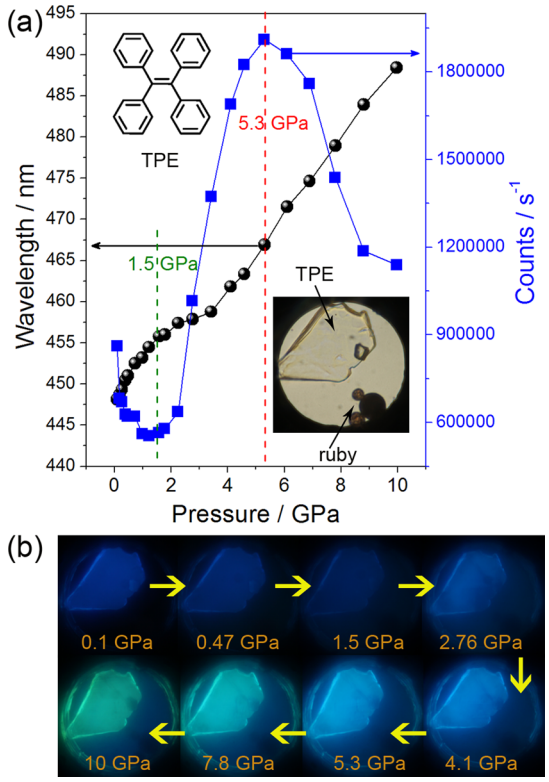

Figure 1. (a) Pressure-dependent PL maximum (left axis) and intensity (right axis) of TPE crystals. The inset of panel a includes the molecular structure of TPE and the optical photograph of TPE crystals in DAC. (b) Corresponding typical photographs under UV irradiation (λ_{ex} = 375 nm).

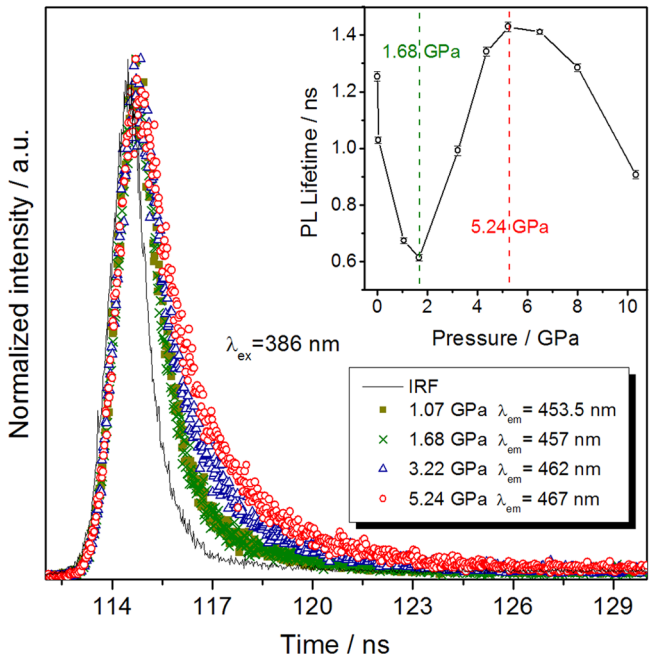

Figure 2. Typical PL decays of TPE powder for pressures below 5.24 GPa. The inset depicts the observed lifetime as a function of pressure. IRF: instrumental response function.

As we will see later, this greater red shift is attributed to the deformation of the C−H···π and C−H···C network, which has consequences on the PL efficiency upon compression. Moreover, previous reports have showed that TPE is irresponsive to the mechanical grinding due to its spontaneous crystallization.[11] The distinct luminescence responses to the stresses suggest that the aromatic C−H···π and C−H···C contacts are strong enough to stabilize molecule packing styles under mechanical grinding but mutable to extreme pressure. Notably, a drastic emission enhancement was observed in the pressure range of 1.5−5.3 GPa, in contrast with the emission decrease in the other two pressure ranges, 0.1 to 1.5 GPa and 5.3−10 GPa. The maximum PL intensity (λ_{em} = 467 nm) at 5.3 GPa is about three times that (λ_{em} = 455.8 nm) at 1.5 GPa (Figure 1a). The pressure-dependent color and intensity change could be readily visualized by naked eye as well (Figure 1b). The remarkable emission enhancement is highly reproducible for both TPE crystals and powder in a comparable pressure range (Figures S3−S6, Supporting Information). When pressure was gradually released to ambient conditions, the PL spectra turned back to the original emission band. This reversible pressure-dependent PL change illustrates the role of aromatic C−H···π and C−H···C contacts in the structural recovery.

To further validate the abnormal pressure-dependent emission change, we performed PL decays of TPE powder for pressures of 0.1 MPa to 10.33 GPa (Figure 2 and Figure S8, Supporting Information). The fluorescence decay profiles were analyzed using the PTI's FeliX32 software package. The goodness of the decay fits was assessed by considering the reduced chi square (χ^2) value and the randomness of the weighted residuals, in which the monoexponential fits were well acceptable for the decay profiles with various pressures (Figure S9, Supporting Information). The PL lifetime data are summarized in the inset of Figure 2. (The instrument limit is 0.1 ns.) The change of lifetime coincided well with the change of PL intensity. In particular, the lifetime increased promptly with the elevated pressure from 1.68 to 5.24 GPa, verifying the direct observation of the emission enhancement in a comparable pressure range. It is worth noting that the pressure-dependent PL intensity and lifetime change in TPE is abundant and extraordinary, which is seldom reported.

To gain insight into this distinctive emission change, high-pressure synchrotron powder X-ray diffraction (XRD) experiments were performed at room temperature. The simulated XRD patterns at room temperature (283−303 K) and low temperature (100 K) determined from the reported single-crystal results are considered as reference.[24,25] According to crystallographic analysis, the aromatic C−H···π and C−H···C contacts are strengthened when the temperature is decreased (Figures S10 and S11 and Table S1, Supporting Information).[24,25] In particular, the H12···C18 distance at 100 K (2.803 Å) is ∼0.10 Å shorter than the sum of van der Waals radii of H and C (1.2 and 1.7 Å, respectively, according to Bondi, 1964).[26] The C16−H12···C18 angle at 100 K is 148.69°, which preferably tends toward 180°. It is suggested that the C16−H12···C18 hydrogen bond is formed at 100 K. Moreover, from high to low temperatures, the *b* axis contracts significantly, while the *a* and *c* axes change limitedly.[27] To verify whether the compression of TPE under pressure would be anisotropic, we performed the Le Bail refinements (Figure S14, Supporting Information). The refinement results indicate that the compression of TPE is anisotropic, with the *b* axis being the most compressible axis (Table S2, Supporting Information). One can estimate this anisotropic compression by tracing the relative positions of the Bragg peaks indexed in Figure 3. For

dx.doi.org/10.1021/jz501371k | J. Phys. Chem. Lett. 2014, 5, 2968−2973

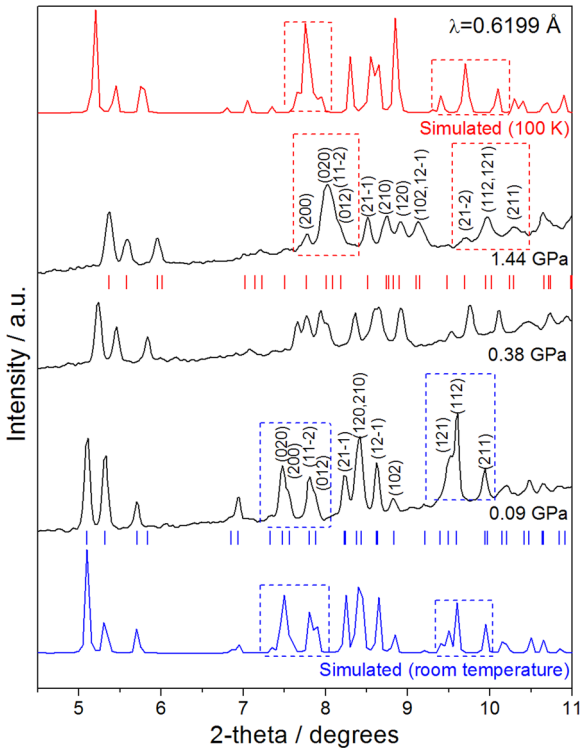

Figure 3. XRD patterns of TPE at low pressures (λ = 0.6199 Å). The simulated patterns at room temperature and 100 K are shown in blue and red, respectively. The characteristic Bragg peaks are indexed based on the structural refinements. The vertical ticks indicate the calculated positions for Bragg reflections. The fingerprint regions are marked by relevant frameworks.

example, the Bragg peak (020) moves faster than the Bragg peak (200) with increasing pressure. It is worth noting that the unit-cell contraction at 1.44 GPa/300 K is more significant than that at 0.1 MPa/100 K, while the PL shift at 0.1 MPa/100 K is much larger than that at 1.44 GPa/300 K (Figure S15 and S16, Supporting Information). Given the rigid phenyl and olefinic moieties of TPE molecules, the results allow us to conclude that pressure-induced unit-cell contraction in TPE is dominated by the significant decrease in intermolecular distance rather than the conformational planarization. The intermolecular forces at 1.44 GPa/300 K are thus strengthened much greater than those at 0.1 MPa/100 K. Consequently, it is reasonable to elucidate the pressure-induced enhancement of the C−H···π and C−H···C contacts in compressed TPE, even formation and further strengthening of the relevant hydrogen bonds beyond 1.44 GPa. It can be expected that further high-pressure single X-ray or neutron diffraction measurements would be helpful to give precise structural information on compressed TPE at low pressures.

In general, pressure-induced molecular planarization gives rise to an increased oscillator strength, contributing to a PL intensity and lifetime decrease at high pressures.[14,15] Previous report on metal chelates Alq_3, Gaq_3, and Inq_3 (q = 8-hydroxyquinoline) showed that the faster PL rate under pressure should be correlated to an enhancement of excitation transfer, a consequence of pressure-promoted intermolecular interactions.[15] For conjugated polymer poly(9,9-di-*n*-octylfluorene-*alt*-benzothiadiazole), a greater change in PL decay rate in thin films than solid-solutions is clearly observed, suggesting that the closer intermolecular interactions allow for additional nonradiative decay channels under pressure.[14] Accordingly, the decrease in PL intensity and lifetime of compressed TPE in 0.1 to 1.5 GPa could be explained by bearing these detrimental effects. In light of the restriction of intramolecular rotation (RIR) hypothesis for the mechanism of AIEE phenomenon in propeller-shaped luminogens, the intermolecular interactions lead to the restriction of the aromatic parts movement, which reduces the energy loss through the nonradiative rotational relaxation channel and thus enhances the PL efficiency.[27−29] Combining with the structure analysis, we deduce that the formation and further strengthening of the relevant hydrogen bonds above 1.44 GPa can dampen or restrict the aromatic parts movement more significantly; consequently, the energy loss through the intramolecular motions can be suppressed more efficiently by the enhanced intermolecular interactions in the pressure range of 1.5−5.3 GPa, fading the detrimental effects to PL emission. The XRD patterns beyond 5.3 GPa became blurry, hinting emergence of an amorphous phase, which is likely associated with the emission decrease in the higher pressure range (Figure S13, Supporting Information). Subsequent IR analysis will shed light on this phenomenon.

In addition to XRD measurements, vibrational spectroscopy can provide chemical bonding and local structural information. The high-pressure infrared (IR) measurements were carried out in the pressure range of 0.1 MPa to 10.6 GPa (Figure S17, Supporting Information). The wide IR absorption band around 3060 cm^{-1} could be readily assigned to the aromatic C−H stretching vibration ν(aromatic C−H). A blue shift of the aromatic C−H stretching frequency is observed up to 10.6 GPa, which illustrates the shortening of the aromatic C−H bonds (Figure 4). This blue-shift behavior is characteristic for the formation of weak hydrogen bonds, especially in the case of benzene dimer.[30] It is suggested that the phenyl part might push the C−H hydrogen toward the carbon, which can be explained in terms of an enhancement and modification of these C−H···π contacts with increasing pressure. In the fingerprint region, the bands at 761 and 699 cm^{-1} can be ascribed to out-of-plane C−H bending γ(C−H) and out-of-plane ring deformation ϕ(C−C) vibrations, respectively.[31,32] These two vibrational modes were gradually split and broadened beyond 4.5 GPa, which implies the deformation of the C−H···π and C−H···C network. It is consistent with the XRD result that an amorphous phase emerges beyond 5.3 GPa. As we previously presented, the conformational planarization is augmented when pressure is over ∼4 GPa. Therefore, increasing repulsive and steric stresses induced by higher pressure can be accommodated by the pronounced conformational planarization via deformation of the C−H···π and C−H···C network. It can be imagined that the intermolecular forces in the amorphous phase might be not as effective as those in the crystalline state to restrict the intramolecular rotations, and thereby the PL efficiency at higher pressures could be reduced. Further excessive compression may lead to close interactions of the panel parts of the molecules in the amorphous state, quenching the excited states, which should be correlated to the emission decrease in higher pressure range. Although the latter effect is technically difficult to identify, subsequent IR results on the samples quenched from higher pressures (>10 GPa) provide strong evidence on it.

Previous experimental and theoretical studies by Bini and coworkers have established that pressure-induced ring-opening reaction in benzene can be triggered only when the nearest intermolecular C···C distance approaches ∼2.6 Å.[33,34] This

dx.doi.org/10.1021/jz501371k | J. Phys. Chem. Lett. 2014, 5, 2968−2973

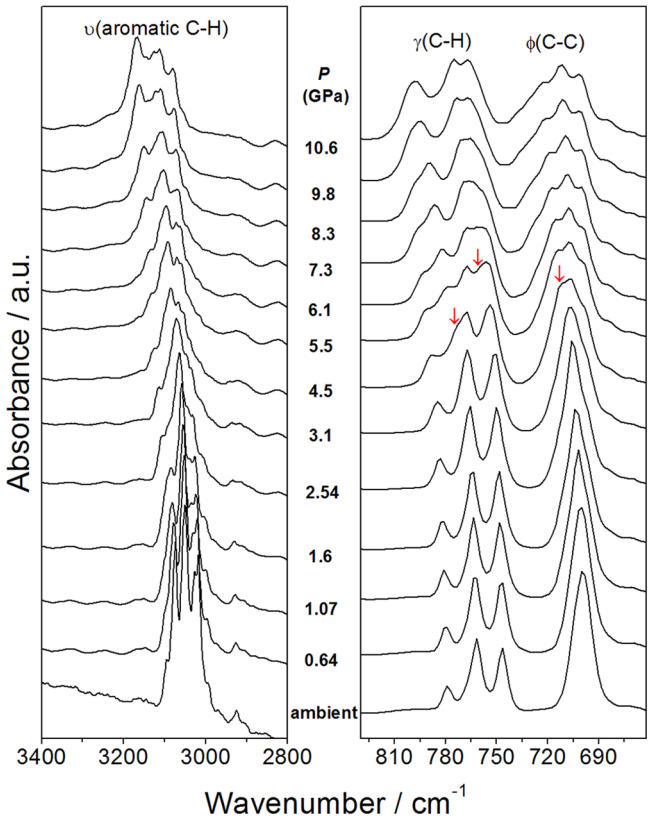

Figure 4. High-pressure IR spectra of TPE in region of ν(C−H), γ(C−H), and ϕ(C−C) vibration modes. The arrows indicate the new peaks.

critical C···C distance (2.6 Å) is ∼25% decreased with respect to the C···C van der Waals contact (3.4 Å).[26,34] When pressure gradually comes to the reaction threshold (∼25 GPa, room temperature), the adjacent rigid benzenes tend to be more parallel and closer to each other, and hence the $\pi-\pi$ intermolecular interactions are maximized accordingly. Motivated by this, we verify whether the ring-opening reaction could occur in highly compressed TPE. As shown in Figure 5, the IR spectra of the TPE samples quenched from 10.6, 13.8, 19.7, and 25.4 GPa were recorded. A broad band at lower frequency relative to aromatic C−H stretching vibration ν(aromatic C−H) emerges and becomes more and more pronounced in the samples recovered from 13.8 to 25.4 GPa. This broad band centered at ∼2920 cm^{-1} can be ambiguously assigned to sp^3 C−H stretching vibration $\nu(sp^3$ C−H), which is the direct evidence to support the ring-opening reaction.[33] In addition, the formation of the excimeric species (parallel configuration) is proved to be the first stage of the ring-opening reaction in compressed benzene.[35] These excimeric species in crystalline benzene steeply increase above 5 GPa, which is much lower than the reaction threshold ∼25 GPa.[33,35] As such, it can be concluded that there should be close interactions of panel parts, such as the formation of the excimeric species in the amorphous TPE upon compression, serving as the nuclei of the chemical reaction. More importantly, these close interactions of relevant panel parts in amorphous TPE are responsible for the emission decrease observed above 5.3 GPa. As seen in Figure 5, the original IR modes can be clearly detected in the quenched samples up to 25.4 GPa. It implies that the unreacted TPE molecules can be reconstructed to a cystalline state basically the same as the original one when pressure is released to ambient conditions, further verifying the role of aromatic C−H···π and C−H···C contacts in the structural recovery. The normalized PL spectra of the corresponding quenched samples were recorded in Figure S18, Supporting Information. With respect to the original PL emission, a broad red-shift emission band was found in the samples recovered from the pressures greater than 13.8 GPa. Given the complexity of the reacted amorphous polymeric products, we infer that the reacted matrix might cause a somewhat distorted molecular structure responding to the emission changes.

In summary, we demonstrate the distinctive luminescence response of TPE to extreme compression. The pressure-promoted intermolecular interactions could lead to an enhancement of excitation transfer and allow for additional nonradiative decay channels, reducing the PL efficiency. However, the formation and further strengthening of the

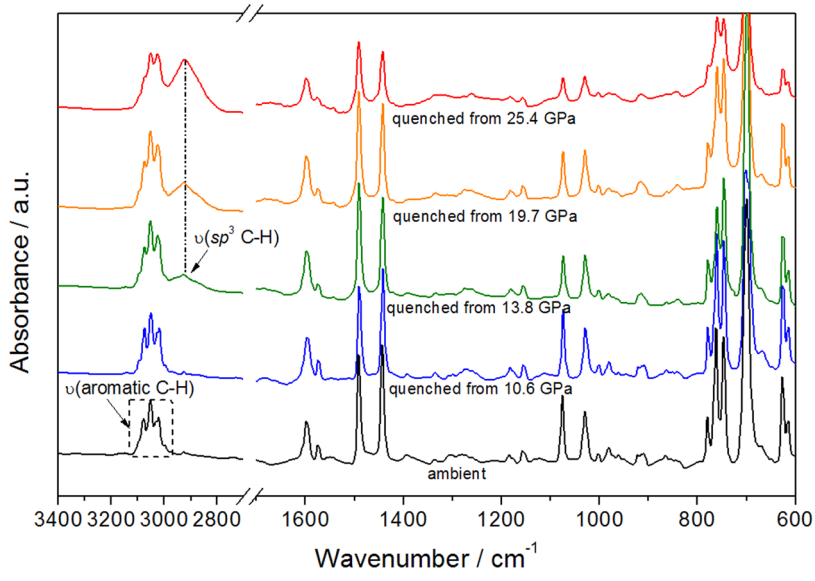

Figure 5. IR spectra of TPE samples under ambient conditions and quenched from 10.6, 13.8, 19.7, and 25.4 GPa.

dx.doi.org/10.1021/jz501371k | J. Phys. Chem. Lett. 2014, 5, 2968−2973

relevant hydrogen bonds beyond 1.44 GPa can dampen or restrict the aromatic parts movement more significantly, suppressing the energy loss through the intramolecular motions and boosting the PL efficiency. The latter effect is dominant in the pressure range of 1.5−5.3 GPa, where a drastic emission enhancement is detected. Further compression will give rise to the deformation of the C−H···π and C−H···C network associated with the amorphization process. Accordingly, the RIR is weakened, and the close interaction of the relevant panel parts (such as the formation of the excimeric species) becomes favorable, quenching the excited states, which is correlated to the emission decrease in higher pressure range (>5.3 GPa). In addition, the reversible PL and IR spectra up to 10 GPa illustrate the role of the intermolecular interactions in the structural recovery. The close correlation between PL and IR spectra changes with increasing pressure reveals that the deformation of the C−H···π and C−H···C network gives rise to a pronounced conformational planarization, resulting in a greater red shift observed in the PL spectra beyond ∼4 GPa. Our study would provide important information on the role of the weak intermolecular interactions in the luminescence properties of AIEE-active luminogens.

EXPERIMENTAL METHODS

Sample Preparation and High-Pressure Generation. TPE powder was purchased from Aldrich (98%), and the fine crystals were obtained by slow evaporation from its acetonitrile solution. The high-pressure experiments were performed using DAC technique with the low-fluorescence diamonds. In general, the powder or crystal sample was placed in the holes (diameter: 200 μm) of a T301 steel gasket, which was preindented to a thickness of 50 μm. Small ruby balls were inserted into the sample compartment for in situ pressure calibration according to the R1 ruby fluorescence method.[36] In the steady-state PL spectra, lifetime decay, and powder XRD experiments, the pressure-transition medium (PTM) was 150 cst silicone oil (Aldrich), providing good hydrostatic conditions and avoiding the possible interaction between the sample and the hydrostatic liquid (Figures S1−S6, Supporting Information). As to IR experiments, KBr was used as the PTM.

PL and Optical Measurements. In situ steady-state PL measurements under high pressure were performed with a QuantaMaster-40 spectrometer (produced by Photon Technology) coupled to an inverted fluorescence microscope (Nikon Ti−U) in reflection mode. The UV irradiation with the excitation wavelength of 375 nm was used as the excitation source. The typical resolution in the present study was 0.25 nm. Optical photographs of the compressed TPE samples were obtained using an imaging camera (Canon EOS 5D Mark II) equipped on the fluorescence microscope. The camera can record the photographs under the same conditions including exposure time and intensity.

Time-Resolved Emission Decay Measurements. High-pressure PL lifetime measurements were performed with a LaserStrobe spectrofluorometer (produced by Photon Technology) coupled to an inverted fluorescence microscope (Nikon Ti−U). The illumination source is a nitrogen pumped dye laser. The laser is triggered by the software/interface with the repetition rate up to 20 Hz. The excitation wavelength of 386 nm is generated by means of the laser dye 4,4‴-bis[(2-butyloctyl)oxy]-1 (purchased from Exciton) toluene/ethanol solvent (in addition to the nitrogen line at 337.1 nm). The optical pulse from the dye laser is fed by a single optical fiber to the sample in DAC through the fluorescence microscope; then, the fluorescence is fed by another single optical fiber to the detector. We would like to point out that "the magic" moment of time equal to ∼115 ns in our high-pressure measurements is caused by pulse delay via the optical fiber we used, but it will not influence the final results. The high-pressure PL time-resolved emission decays were recorded at the corresponding wavelength derived from the high-pressure steady-state data (Figure S8, Supporting Information).

XRD Measurements. In situ high-pressure angle-dispersive XRD experiments with a wavelength of 0.6199 Å and a focused beam size of about 4 × 7 μm^2 were performed at beamline 15U1, Shanghai Synchrotron Radiation Facility (SSRF), China. The XRD patterns were collected for 10 s at each pressure using a Mar-165 CCD detector and then were integrated with FIT2D program.[37]

IR Measurements. IR microspectroscopy of TPE in the crystalline state was carried out with a Bruker Vertex80 V FTIR spectrometer. The samples were measured in a DAC, equipped with type-II cut diamonds with 330 μm culets and a T301 gasket with a hole diameter 120 μm. KBr was used as the PTM.

ASSOCIATED CONTENT

Supporting Information

Experimental procedures, structures, additional PL, IR spectra, and XRD results. This material is available free of charge via the Internet at http://pubs.acs.org.

AUTHOR INFORMATION

Corresponding Author

*E-mail: zoubo@jlu.edu.cn.

Author Contributions

H.Y. and B.Z. designed and performed experiments and analyzed data. K.W., K.Y., and B.L. assisted in performing experiments. K.W. and B. Z. provided intellectual input. H.Y., K.W., and B.Z. wrote the manuscript.

Notes

The authors declare no competing financial interest.

ACKNOWLEDGMENTS

The authors would like to thank Ligong Zhang, Dongxu Zhao, and Haiyang Xu for their help with the low-temperature photoluminescence measurements. The authors would like to acknowledge the useful comments of the reviewers. This work is supported by NSFC (Nos. 91227202 and 11204101), RFDP (No. 20120061130006), National Basic Research Program of China (No. 2011CB808200) and China Postdoctoral Science Foundation (No. 2012M511327). Angle-dispersive XRD measurement was performed at beamline 15U1 at the Shanghai Synchrotron Radiation Facility (SSRF).

REFERENCES

(1) Dong, Y.; Xu, B.; Zhang, J.; Tan, X.; Wang, L.; Chen, J.; Lv, H.; Wen, S.; Li, B.; Ye, L.; Zou, B.; Tian, W. Piezochromic Luminescence Based on the Molecular Aggregation of 9,10-Bis((E)-2-(pyrid-2-yl)vinyl)anthracene. *Angew. Chem., Int. Ed.* **2012**, *51*, 10782−10785.

(2) Yoon, S.; Chung, J.; Gierschner, J.; Kim, K.; Choi, M.; Kim, D.; Park, S. Multistimuli Two-Color Luminescence Switching via Different Slip-Stacking of Highly Fluorescent Molecular Sheets. *J. Am. Chem. Soc.* **2010**, *132*, 13675−13683.

(3) Nagura, K.; Saito, S.; Yusa, H.; Yamawaki, H.; Fujihisa, H.; Sato, H.; Shimoikeda, Y.; Yamaguchi, S. Distinct Responses to Mechanical

Grinding and Hydrostatic Pressure in Luminescent Chromism of Tetrathiazolylthiophene. *J. Am. Chem. Soc.* **2013**, *135*, 10322−10325.
(4) Gierschner, J.; Lüer, G.; Milián-Medina, B.; Oelkrug, D.; Egelhaaf, H. Highly Emissive H-Aggregates or Aggregation-Induced Emission Quenching? The Photophysics of All-Trans para-Distyrylbenzene. *J. Phys. Chem. Lett.* **2013**, *4*, 2686−2697.
(5) Mutai, T.; Satou, H.; Araki, K. Reproducible On−Off Switching of Solid-State Luminescence by Controlling Molecular Packing through Heat-Mode Interconversion. *Nat. Mater.* **2005**, *4*, 685−687.
(6) An, B.; Kwon, S.; Jung, S.; Park, S. Enhanced Emission and Its Switching in Fluorescent Organic Nanoparticles. *J. Am. Chem. Soc.* **2002**, *124*, 14410−14415.
(7) An, B.; Lee, D.; Lee, J.; Park, Y.; Song, H.; Park, S. Strongly Fluorescent Organogel System Comprising Fibrillar Self-Assembly of a Trifluoromethyl-Based Cyanostilbene Derivative. *J. Am. Chem. Soc.* **2004**, *126*, 10232−10233.
(8) Hong, Y.; Lam, J.; Tang, B. Aggregation-Induced Emission: Phenomenon, Mechanism and Applications. *Chem. Commun.* **2009**, *29*, 4332−4353.
(9) Hong, Y.; Lam, J.; Tang, B. Aggregation-Induced Emission. *Chem. Soc. Rev.* **2011**, *40*, 5361−5388.
(10) Zhao, N.; Yang, Z.; Lam, J.; Sung, H.; Xie, N.; Chen, S.; Su, H.; Gao, M.; Williams, I.; Wong, K.; Tang, B. Benzothiazolium-Functionalized Tetraphenylethene: An AIE Luminogens with Tunable Solid-State Emission. *Chem. Commun.* **2012**, *48*, 8637−8639.
(11) Shi, J.; Chang, N.; Li, C.; Mei, J.; Deng, C.; Luo, X.; Liu, Z.; Bo, Z.; Dong, Y.; Tang, B. Locking The Phenyl Rings Of Tetraphenylethene Step by Step: Understanding The Mechanism of Aggregation-Induced Emission. *Chem. Commun.* **2012**, *48*, 10675−10677.
(12) Yuan, W.; Tan, Y.; Gong, Y.; Lu, P.; Lam, J.; Shen, X.; Feng, C.; Sung, H.; Lu, Y.; Williams, I. D.; Sun, J.; Zhang, Y.; Tang, B. Synergy between Twisted Conformation and Effective Intermolecular Interactions: Strategy for Efficient Mechanochromic Luminogens with High Contrast. *Adv. Mater.* **2013**, *25*, 2837−2843.
(13) Yuan, W.; Shen, X.; Zhao, H.; Lam, J.; Tang, L.; Lu, P.; Wang, C.; Liu, Y.; Wang, Z.; Zheng, Q.; Sun, J.; Ma, Y.; Tang, B. Crystallization-Induced Phosphorescence of Pure Organic Luminogens at Room Temperature. *J. Phys. Chem. C* **2010**, *114*, 6090−6099.
(14) Schmidtke, J. P.; Kim, J.; Gierschner, J.; Silva, C.; Friend, R. H. Optical Spectroscopy of A Polyfluorene Copolymer at High Pressure: Intra- and Intermolecular Interactions. *Phys. Rev. Lett.* **2007**, *99*, 167401.
(15) Hernández, I.; Gillin, W. P. Influence of High Hydrostatic Pressure on Alq3, Gaq3, and Inq3 (q= 8-Hydroxyquinoline). *J. Phys. Chem. B* **2009**, *113*, 14079−14086.
(16) Dreger, Z. A.; Balasubramaniam, E.; Gupta, Y. M. High-Pressure Effects on the Electronic Structure of Anthracence Single Crystals: Role of Nonhydrostacity. *J. Phys. Chem. A* **2009**, *113*, 1489−1496.
(17) Li, S.; Wang, Q.; Qian, Y.; Wang, S.; Li, Y.; Yang, G. Understanding the Pressure-Induced Emission Enhancement for Triple Fluorescent Compound with Excited-State Intramolecular Proton Transfer. *J. Phys. Chem. A* **2007**, *111*, 11793−11800.
(18) Tan, X.; Wang, K.; Li, S.; Yuan, H.; Yan, T.; Liu, J.; Yang, K.; Liu, B.; Zou, G.; Zou, B. Exploration of the Pyrazinamide Polymorphism at High Pressure. *J. Phys. Chem. B* **2012**, *116*, 14441−14450.
(19) Yan, T.; Wang, K.; Duan, D.; Tan, X.; Liu, B.; Zou, B. P-Aminobenzoic Acid Polymorphs under High Pressures. *RSC Adv.* **2014**, *4*, 15534−15541.
(20) Dziubek, K.; Jęczmiński, D.; Katrusiak, A. Pressure-Generated Hydrogen Bonds and the Role of Subtle Molecular Features in Tetrahydrofuran. *J. Phys. Chem. Lett.* **2010**, *1*, 844−849.
(21) Wang, K.; Duan, D.; Wang, R.; Liu, D.; Tang, L.; Cui, T.; Liu, B.; Cui, Q.; Liu, J.; Zou, B.; Zou, G. Pressure-Induced Phase Transition in Hydrogen-Bonded Supramolecular Adduct Formed by Cyanuric Acid and Melamine. *J. Phys. Chem. B* **2009**, *113*, 14719−14724.
(22) Li, S.; Li, Q.; Zhou, J.; Wang, R.; Jiang, Z.; Wang, K.; Xu, D.; Liu, J.; Liu, B.; Zou, G.; Zou, B. Effect of High Pressure on the Typical Supramolecular Structure of Guanidinium Methanesulfonate. *J. Phys. Chem. B* **2012**, *116*, 3092−3098.
(23) Li, Q.; Li, S.; Wang, K.; Li, X.; Liu, J.; Liu, B.; Zou, G.; Zou, B. Pressure-Induced Isosymmetric Phase Transition in Sulfamic Acid: A Combined Raman and X-Ray Diffraction Study. *J. Chem. Phys.* **2013**, *138*, 214505.
(24) Hua, G.; Li, Y.; A. Slawin, M. Z.; Woollins, J. D. *Dalton Trans.* **2007**, 1477−1480.
(25) Ino, I.; Wu, L.; Munakata, M.; Kuroda-Sowa, T.; Maekawa, M.; Suenaga, Y.; Sakai, R. Bridged Silver(I) Complexes of the Polycyclic Aromatic Compounds Tetraphenylethylene and 1,1,4,4-Tetraphenyl-1,3-butadiene. *Inorg. Chem.* **2000**, *39*, 5430−5436.
(26) Bondi, A. Van Der Waals Volumes and Radii. *J. Phys. Chem.* **1964**, *68*, 441−451.
(27) Parrott, E.; Tan, N.; Hu, R.; Zeitler, J.; Tang, B.; Pickwell-MacPherson, E. Direct Evidence to Support the Restriction of Intramolecular Rotation Hypothesis for the Mechanism of Aggregation-Induced Emission: Temperature Resolved Terahertz Spectra of Tetraphenylethene. *Mater. Horiz.* **2014**, *1*, 251−258.
(28) Virgili, T.; Forni, A.; Cariati, E.; Pasini, D.; Botta, C. Direct Evidence of Torsional Motion in an Aggregation-Induced Emissive Chromophore. *J. Phys. Chem. C* **2013**, *117*, 27161−27166.
(29) Fan, X.; Sun, J.; Wang, F.; Chu, Z.; Wang, P.; Dong, Y.; Hu, R.; Tang, B.; Zou, D. Photoluminescence and Electroluminescence of Hexaphenylsilole are Enhanced by Pressurization in the Solid State. *Chem. Commun.* **2008**, 2989−2991.
(30) Hobza, P.; Zdeněk, H. Blue-Shifting Hydrogen Bonds. *Chem. Rev.* **2000**, *100*, 4253−4264.
(31) Whiffen, D. H. Vibrational Frequencies and Thermodynamic Properties of Fluoro-, Chloro-, Bromo-, And Iodo-Benzene. *J. Chem. Soc.* **1956**, 1350−1356.
(32) Kross, R. D.; Fassel, V. A.; Margoshes, M. The Infrared Spectra of Aromatic Compounds: I. The out-of-Plane CH Bending Vibrations in the Region 625−900 cm^{-1}. *Spectrochimi. Acta* **1956**, *7*, 14−24.
(33) Ciabini, L.; Santoro, M.; Bini, R.; Schettino, V. High Pressure Reactivity of Solid Benzene Probed by Infrared Spectroscopy. *J. Chem. Phys.* **2002**, *116*, 2928−2935.
(34) Ciabini, L.; Santoro, M.; Gorelli, F. A.; Bini, R.; Schettino, V.; Raugei, S. Triggering Dynamics of the High-Pressure Benzene Amorphization. *Nat. Mater.* **2007**, *6*, 39−43.
(35) Citroni, M.; Bini, R.; Foggi, P.; Schettino, V. Role of Excited Electronic States in the High-Pressure Amorphization of Benzene. *Proc. Natl. Acad. Sci. U.S.A.* **2008**, *105*, 7658−7663.
(36) Mao, H. K.; Xu, J.; Bell, P. J. Calibration of the Ruby Pressure Gauge to 800 Kbar under Quasi-Hydrostatic Conditions. *J. Geophys. Res.* **1986**, *91*, 4673−4676.
(37) Hammersley, A.; Svensson, S.; Hanfland, M.; Fitch, A.; Hausermann, D. Two-Dimensional Detector Software: from Real Detector to Idealised Image or Two-Theta Scan. *High Pressure Res.* **1996**, *14*, 235−248.